Fine Structure of Type-I Edge-Localized Modes in the Steep Gradient Region

B. Kurzan,* H. D. Murmann, and J. Neuhauser

(ASDEX Upgrade Team)

Max-Planck-Institut für Plasmaphysik, EURATOM Association, Boltzmannstr. 2, D-85748 Garching, Germany
(Received 3 September 2004; published 26 September 2005)

Fast, high resolution multichannel Thomson scattering is used to quantitatively determine plasma perturbations induced by type-I edge-localized modes (ELMs) in the low-field side edge of ASDEX Upgrade *H*-mode plasmas. 2D snapshots of temperature and density, deduced from the laser light scattered in a vertically elongated, poloidal array of 5×10 scattering volumes, are obtained in the hot, steep edge gradient zone, which is difficult to access by other diagnostics. Local maxima and minima with large amplitude are identified during ELMs and even in the precursor phase, both in density and temperature. Interpreting these structures as footprints of approximately field aligned helical modes in accordance with previous experimental and theoretical work, toroidal mode numbers between 8 and 20 are obtained, roughly consistent with corresponding scrape-off layer and divertor measurements.

DOI: 10.1103/PhysRevLett.95.145001 PACS numbers: 52.55.Dy

The transient first wall power load caused by type-I edge-localized modes (ELMs) [1] in high performance H-mode [2] plasmas is a critical issue for next step magnetic confinement fusion experiments. Accordingly, significant effort has been and still is devoted to experimental ELM analysis on all major tokamaks [see [3] and references therein], and to the development of theoretical ELM models [4,5]. Though multifaceted in detail, a common ELM feature is the observation of magnetic field aligned filamentary structures, probably originating from the hot edge pedestal region and moving outward, transporting particles and energy rapidly into the scrape-off layer (SOL). Experimentally, the resulting average, ELM induced edge profile modifications can be routinely followed over the whole edge region by standard 1D radial profile diagnostics like Thomson scattering [3,6,7], reflectometry [8,9], electron cyclotron emission, etc. It is, however, much more difficult to resolve the nonaxisymmetric filamentary structures, their origin, and time evolution in sufficient detail. On the DIII-D tokamak the fine structure of ELMs in the SOL was resolved by Langmuir probes and interpreted as filaments [10] for the first time. On ASDEX Upgrade, helical structures (or their footprints, respectively) have been clearly identified on first wall structures, e.g., by fast 2D thermography on divertor targets [11] and low-field side limiters [12], and in the low-field side SOL by Langmuir probes [13,14]. The latter have been compared also with the ELM characteristics found in the spherical tokamak MAST, and the similarities and differences have been discussed in the light of evolving theories [see references in [14] for more details].

In this Letter we demonstrate that, exploiting the specific features of the ASDEX Upgrade Thomson scattering system, these first wall and SOL related results can be complemented by a quantitative analysis of the ELM perturbations in the hot pedestal region near and inside the separatrix. During type-I ELMs localized maxima and corresponding minima (''blobs'' and ''holes'') in the electron density and temperature are clearly visible in the steep gradient region inside the separatrix on 2D images, obtained in a poloidal plane by the ASDEX Upgrade vertical Thomson scattering system [15]. This Thomson scattering diagnostic consists of a bundle of up to six vertically launched, radially staggered Nd-YAG laser beams. The scattered light is observed from the low-field side in 16 spatial channels with one optical detection system per channel only. The radial resolution is retained by firing the radially staggered lasers one after the other. Altogether, this arrangement forms a 2D matrix of scattering volumes in a poloidal cross section. With the recently installed ultrafast transient recorders for data acquisition it is now possible to reduce the time delay between lasers down to 500 ns, and, in addition, the accuracy of the measured data is much increased due to improved background noise treatment [16]. The whole system can be shifted radially to measure core or, as in the present Letter, edge plasma profiles and structures. For this study of the plasma edge, 5 Nd-YAG lasers (repetition rate 20 Hz, pulse energy 0.7 J) were available, each with about 1.5 mm beam diameter (Fig. 1). The radial spacing between adjacent laser beams was 2.7 mm. The extent of each scattering volume along the laser beam in vertical direction was 25 mm, and the distance between the centers of vertically adjacent volumes was 60 mm. With the YAG system positioned at the edge only the upper 10 channels give useful plasma information. Altogether this forms a vertically stretched (R, z) matrix of 5×10 scattering volumes, covering a 2D field at the plasma edge with 53 cm in vertical and 1.1 cm in radial direction (see zoom in Fig. 1). The vertical elongation of individual scattering volumes (and of the full matrix) is

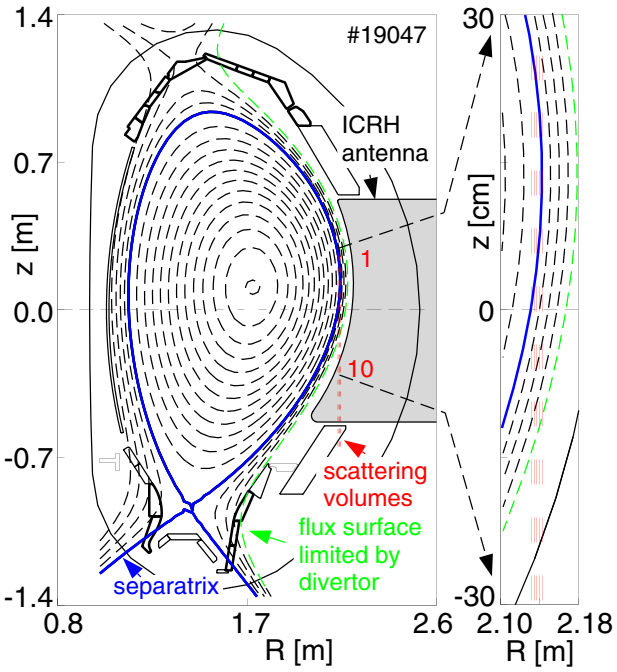

FIG. 1 (color online). Poloidal cross section of ASDEX Upgrade with lower single null magnetic equilibrium. The positions of the scattering volumes of the vertical Thomson scattering system are indicated both in the left part of the figure and in the zoomed up detail in the right part. The separatrix and the outermost open flux surface limited by the divertor are marked. The guard limiter of the ICRH antenna acts as a second limiter.

well suited for investigations of the quiescent plasma edge, because they are roughly aligned parallel to the flux surfaces, where electron density and temperature are constant. But even for the observation of field aligned mode structures, the number, size, and orientation of the scattering volumes on the low-field side of the tokamak is favorable, because the shape of MHD modes on the low-field side is strongly elongated in the poloidal direction.

To study fast plasma events like type-I ELMs, lasting for about 1 ms, all 5 lasers are fired in burst mode: the time between firing the first, innermost laser and the last, outermost laser is 2 μs. This time resolution is fast enough to investigate the dynamics during a type-I ELM in ASDEX Upgrade, because fast moving fine structures of the energy deposition in the divertor during an ELM could already be resolved in ASDEX Upgrade with a shutter speed of 20 μs [11]. The laser bursts are repeated every 50 ms for the 20 Hz lasers. With the new data processing technique [16], which is used now, hardly any artefacts are generated in the evaluated electron density and temperatures. The probability for generating outliers, which deviate by more than 3 standard deviations from an ensemble of data, is less than 1.5%. The relative statistical errors for electron densities $n_e \geq 5 \times 10^{18}$ m^{-3} are $\Delta n_e/n_e \leq 10\%$ and $\Delta T_e/T_e \leq 15\%$. The relative systematic errors due to calibration errors and alignment are $\Delta n_e/n_e \lesssim 7\%$ and $\Delta T_e/T_e \approx 5\%$.

The type-I ELMs are investigated for a deuterium plasma with a lower single null magnetic configuration (Fig. 1). Mapped to the midplane, the outer divertor baffle position is about 3.6 cm outside the separatrix. The ion cyclotron resonance heating (ICRH) antenna guard limiters are 6 cm away from the separatrix. Usually, no significant electron density and temperature values are obtained in the shadow of the ICRH antenna limiters. This means that the electron densities in this region are below the electron density value $n_e \leq 3 \times 10^{17}$ m^{-3}, which can still be determined with a signal-to-noise ratio of 1.

The parameters of the discharges #19046 and #19047, which are investigated mainly in this Letter, are: toroidal magnetic field $B_t = -3.0$ T, plasma current $I_p = 800$ kA, safety factor $q_{95} = 7.5$, line-averaged density $\bar{n}_e = 5 \times 10^{19}$ m^{-3}, heating power by neutral beam coinjection $P_{\mathrm{NBI}} = 7.8$ MW, elongation $\kappa = 1.82$, upper triangularity $\delta_u = 0.24$, lower triangularity $\delta_l = 0.45$, rather similar to those in [14].

The electron density and temperature values measured locally in the poloidal plane during an ''exposure time'' of 2 μs (duration of a laser burst sequence) are presented in the following in the form of contour plots. If the error of measurement is larger than the actual measured value, the data point is set to zero. This is done to improve the significance of the plotted data. The radial coordinate in the plots is the major radius R minus the outermost position R_{out} of the separatrix on the low-field side.

A quiescent phase 10 ms before the ELM as marked in the time trace of the D_α signal (Fig. 2) is used to check the accuracy of the determined electron density and temperatures. A contour plot of the poloidal flux (dashed black lines) is overlaid, indicating the poloidal cross section of the flux surfaces. The poloidal flux increment between contour lines is 0.05 Vs, corresponding to an increment of 0.02 in the normalized poloidal flux coordinate ρ_{pol}. The error in the radial position of the separatrix, obtained by the equilibrium code CLISTE [17], is about 5 mm.

The deviations between the contours of constant electron density and temperature and the shape of the flux surfaces, as determined by equilibrium reconstruction from magnetic signals, are within the systematic errors of the measured electron densities and temperatures.

At a time of 0.58 ms before the ELM (Fig. 3) the contours of constant electron density show local blob structures along a flux surface around the separatrix. The blobs in the electron density are not due to the systematic errors in the measurement of the electron density, which are visible in Fig. 2. These structures also cannot be explained by statistical fluctuations. Within the two blobs the electron density extends over 3 scattering volumes each. It is very unlikely that these 6 data points are caused either by 6 outliers having the same value, or by the statistical errors of the data, which must be ordered such, that two plateaus are formed in a gradient region of the plasma. These blob structures are therefore significant.

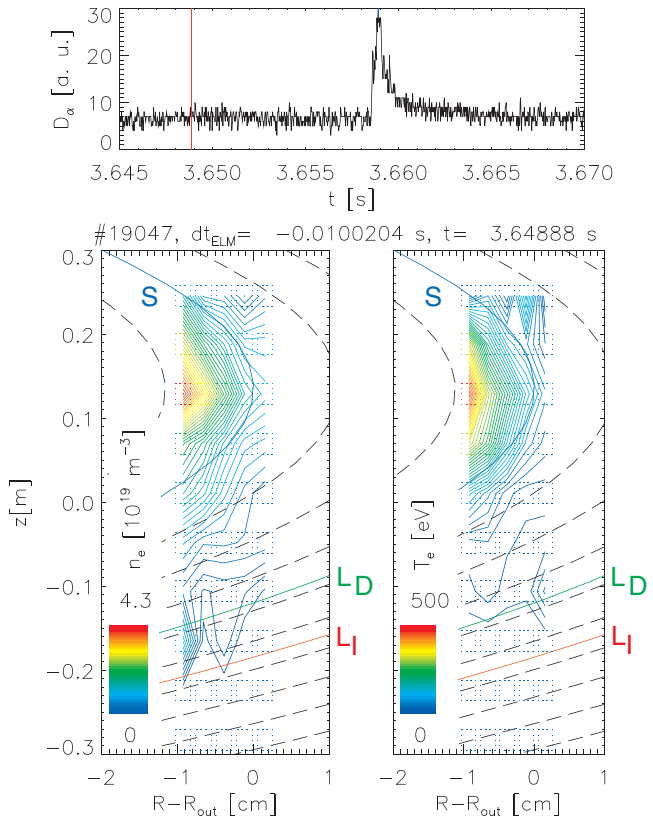

FIG. 2 (color). Electron density and temperature contours in a quiescent phase 10 ms before an ELM. This time point is marked by a vertical line in the D_α trace. The contour lines follow closely the overlaid flux surfaces determined by equilibrium reconstruction from magnetics. The separatrix (S), and the flux surfaces, which are tangent to the divertor (L_D), and the ICRH antenna (L_I) are marked. The scattering volumes are marked by dotted rectangulars.

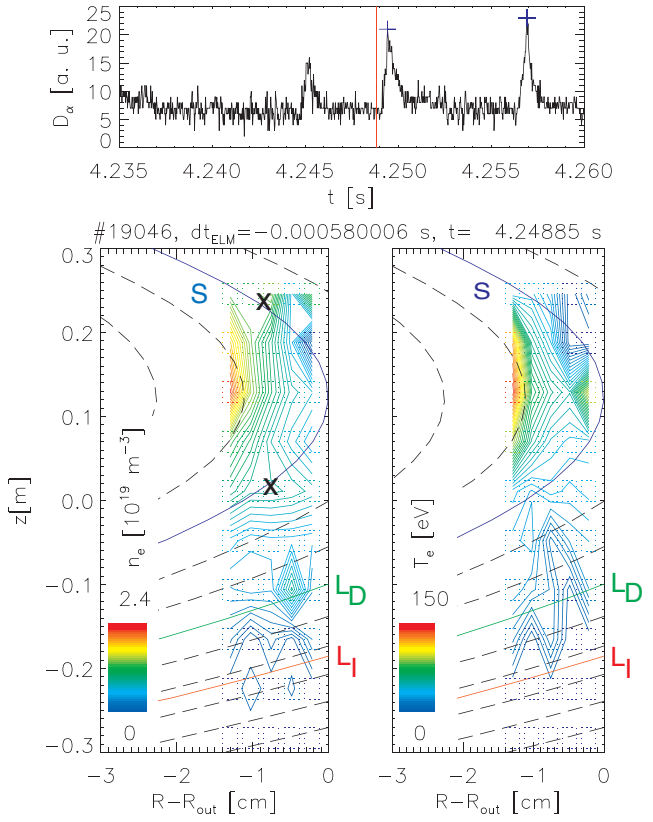

FIG. 3 (color). Electron density and temperature contours 0.58 ms before an ELM in the poloidal plane of the plasma. The symbols have the same meaning as in Fig. 2, but note the different scales. Blob structures, marked by the symbol ×, are seen in the electron density near the separatrix. They can be interpreted as a helical structure with $n \approx 10$. The other fine structures in the electron density and temperature might be due to smaller scale plasma fluctuations.

Interpreting these structures as footprints of field aligned helical structures on a poloidal plane, an effective toroidal mode number n can be estimated: given the measured poloidal wavelength (distance between two poloidally adjacent maxima) and the magnetic pitch angle, the corresponding toroidal wavelength can be determined, with n the number of periods on a toroidal circumference. One should notice that these transient helical structures are not coherent modes and therefore n as defined above is not necessarily an integer. For the blob structure seen before the ELM (Fig. 3) this effective toroidal mode number is $n \approx 10$. Up to now such blobs have been observed up to 1.4 ms before the ELM and always at the same spatial position. They are therefore interpreted as locked ELM precursors [18]. In a similar discharge, but with $B_t = -2.5$ T and $I_p = 1.0$ MA (#19812) a precursor with $n \approx 9$ was found.

It must be noted that only structures in the range $8 \leq n \leq 40$ can be identified. For modes with $n < 8$ only a single blob at most would be seen in the area covered by the Thomson scattering system, making it impossible to determine n. Such a single blob, however, has not yet been observed. The upper limit is determined by the spatial resolution.

In a phase 113 μs after a maximum in the D_α intensity the difference $\Delta p_e = -290$ Pa between the pedestal pressure and the mean pedestal pressure, which is averaged in time including ELMs, is strongly negative. In fact, spatially coincident holes are seen in the electron density and temperature in the hot steep gradient region inside the separatrix, which is difficult to explore quantitatively by other diagnostics without massive plasma perturbation. Around and outside the separatrix maxima are seen in a threefold electron density and a twofold electron temperature structure (Fig. 4). When these blobs are again interpreted as helical structures, toroidal mode numbers of $n \approx 20$ and $n \approx 14$ are found for the electron density and the electron temperature, respectively. The maxima of the structure in the electron temperature do not coincide with the positions of maxima in the threefold structure of the electron density. This can mean that the filaments visible as electron density blobs are ''older'' (further

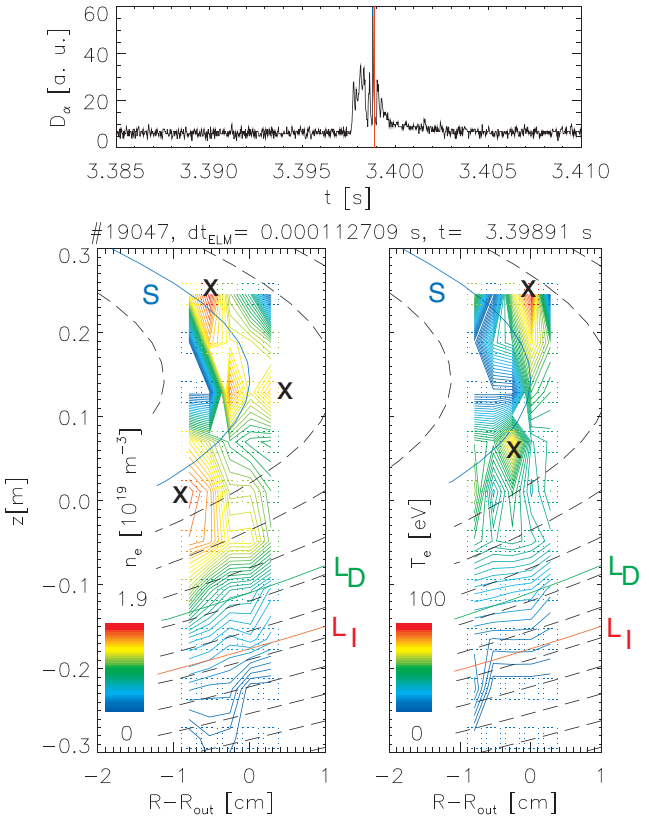

FIG. 4 (color). Electron density and temperature contours 113 μs after the maximum in D_α intensity of an ELM in the poloidal plane of the plasma. The symbols have the same meaning as in Figs. 2 and 3, but note the different scales. A threefold blob structure in the electron density ($n \approx 20$) and a twofold blob structure in the electron temperature outside the separatrix ($n \approx 14$) exist. In addition, inside the separatrix there are spatially coinciding holes of electron density and temperature.

away from the separatrix) and have already lost their electron energy content by fast parallel heat conduction. No density blobs correlated with the electron temperature blobs are observable, because they can be hidden in the minimas between the large density blob structures. Particles and energy from the pedestal have obviously been transported to the blobs around the separatrix, leaving holes further inwards in the hot steep gradient region (Fig. 4). In another discharge (#19807) where the Thomson scattering system was measuring near and inside the separatrix, a twofold structure of holes close to the separatrix, again spatially coincident in temperature and density, is found in between two ELMs with $n \approx 15$. The radial and poloidal diameters of these holes are estimated to be about 1 cm and 8 cm, respectively.

Since spirals of the ELM's filaments are observed outside the separatrix on the divertor plates by thermography [11] apparently a reconnection of the magnetic field lines has taken place and the filaments in the SOL are no longer connected to the main plasma. A theoretical interpretation of the blobs observed in the SOL as nonrotating vertically elongated filaments yields a mean radial outward velocity of between 200 ms^{-1} and 800 ms^{-1} [19]. Such radial velocities as well as typical toroidal and poloidal plasma edge rotation velocities of less than 10 kms^{-1} are small enough to avoid blurring of blob structures during the "exposure time" of 2 μs.

Summarizing, it is found that in ASDEX Upgrade during a type-I ELM blob like structures are observed in the electron density and temperature around the separatrix and in the SOL, while holes are found in the steep gradient region inside the separatrix. When interpreting these blobs as field aligned helical structures toroidal mode numbers between $n \approx 8$–20 are found. This is in good agreement with the toroidal mode numbers found with Langmuir probe measurements [14] in the SOL, and for the nonaxisymmetric energy deposition pattern on the divertor tiles for type-I ELMs in ASDEX Upgrade [11]. Altogether there is clear experimental evidence that at least part of the ELM related filaments have their origin indeed in the hot, steep gradient region as predicted by theory [4].

*Electronic address: Kurzan@ipp.mpg.de

[1] W. Suttrop, Plasma Phys. Controlled Fusion **42**, A1 (2000).
[2] F. Wagner *et al.*, Phys. Rev. Lett. **49**, 1408 (1982).
[3] A. Kirk *et al.*, Phys. Rev. Lett. **92**, 245002 (2004); A. Kirk *et al.*, Plasma Phys. Controlled Fusion **47**, 315 (2005).
[4] J. W. Connor *et al.*, Phys. Plasmas **5**, 2687 (1998).
[5] H. R. Wilson *et al.*, Phys. Rev. Lett. **92**, 175006 (2004).
[6] M. Jakobi *et al.*, Europhysics Conference Abstracts 26B (2002), contribution 1.122.
[7] A. W. Leonard *et al.*, Plasma Phys. Controlled Fusion **44**, 945 (2002).
[8] L. Zeng *et al.*, Plasma Phys. Controlled Fusion **46**, A121 (2004).
[9] I. Nunes *et al.*, Nucl. Fusion **44**, 883 (2004).
[10] D. L. Rudakov *et al.*, Plasma Phys. Controlled Fusion **44**, 717 (2002).
[11] T. Eich *et al.*, Phys. Rev. Lett. **91**, 195003 (2003); T. Eich *et al.*, Plasma Phys. Controlled Fusion **47**, 815 (2005).
[12] A. Herrmann *et al.*, Plasma Phys. Controlled Fusion **46**, 971 (2004).
[13] H. W. Müller *et al.*, Europhysics Conference Abstracts 26B (2002), contribution O-2.06.
[14] A. Kirk *et al.*, Plasma Phys. Controlled Fusion **47**, 995 (2005).
[15] H. D. Murmann *et al.*, Rev. Sci. Instrum. **63**, 4941 (1992).
[16] B. Kurzan *et al.*, Plasma Phys. Controlled Fusion **46**, 299 (2004).
[17] W. Schneider *et al.*, Fusion Eng. Des. **48**, 127 (2000).
[18] T. Bolzonella *et al.*, Plasma Phys. Controlled Fusion **46**, A143 (2004).
[19] S. I. Krasheninnikov *et al.*, Phys. Lett. A **283**, 368 (2001).